Effect of Silica-Particle Characteristics on Impact/Usual Fatigue Properties and Evaluation of Mechanical Characteristics of Silica-Particle Epoxy Resins*

Isamu YAMAMOTO**, Takashi HIGASHIHARA***
and Toshiro KOBAYASHI****

The structure (crystalline or amorphous) and shape (globular or irregular) of silica fillers were varied and their effects on the impact fatigue and usual fatigue properties in the particle-filled epoxy resins were investigated. The fatigue crack extension process was discussed in terms of initiation and propagation processes. Furthermore, the mechanical characteristics of the material were evaluated by considering the tensile properties, fatigue resistance and the fracture behavior. It has been found that the epoxy resin filled with irregular crystalline silica-particles possessed the best combination of mechanical properties.

Key Words: Composite Material, Fatigue, Fracture Toughness, Reinforced Plastics, Silica-Particle-Filled Epoxy Resins, Mechanical Properties

1. Introduction

Silica-filled epoxy resins have been extensively used as package materials of electric and electronics components and structural materials in cases where electrical insulation is required, because of their i) low thermal expansion coefficient (CTE), ii) good thermal conductivity, and iii) improved mechanical properties due to the silica-particle filling.

Many studies concerning mechanical properties and fracture behavior of the silica-filled epoxy resins have been carried out. For example, Nishimura et al. have performed the static strength test, fatigue test and creep test and investigated the relationships among each property for three kinds of fused-silica-particle-filled epoxy resins[1]. In addition, the effects of particle size, distribution and particle shape on the strength and the fracture properties have been investigated by the research group of Nishimura and Yaguchi[2)-4)]. Nakamura et al. have investigated the mechanical characteristics such as Young's modulus, strength, fracture toughness and impact toughness and reported the relationships between particle characteristics and mechanical characteristics for the epoxy resin with irregular-shape silica-particles and that with globular silica-particles[5)-10)].

Kobayashi et al. have also conducted many studies on the silica-filled epoxy resins for the purpose of developing new uses for them including the followings: (1) The dynamic fracture toughness evaluation method using the instrumented Charpy impact test was investigated for various polymers[11)]. (2) Relationship between tensile properties and impact fatigue properties were studied for the irregular crystalline silica-filled epoxy resins[12),13)]. (3) Effects of silica-particle characteristics on the static fracture toughness and the dynamic fracture toughness were studied for the irregular crystalline silica-particle filled epoxy resin, irregular amorphous silica-parti-

* Received 1st October, 2001 (No. 01-4141)
** Course for School Teacher, Osaka Kyoiku University, 4-698-1 Asahigaoka, Kashiwara, Osaka 582-8582, Japan. E-mail: iyama@cc.osaka-kyoiku.ac.jp
*** Takaoka Chemical Co., Ltd., 80 Nagare, Jimokuji-cho, Ama-gun, Aich 490-1111, Japan
**** Departments of Productions Systems Engineering, Toyohashi University of Technology, Toyohashi, Aichi 441-8580, Japan

cle-filled epoxy resin and globular amorphous silica-particle-filled epoxy resin[14].

In this study, effects of the silica-particle characteristics such as crystalline/amorphous and globular/irregular on the impact/usual fatigue properties were investigated for the silica-particle-filled epoxy resin. In addition, the characteristics needed for structural application such as fatigue properties, strength and fracture behavior were investigated and the mechanical characteristics were evaluated synthetically.

2. Experimental Procedure

2.1 Material

Four different materials were prepared for this study. Material A is epoxy resin without silica-particles. The irregular crystalline silica-particles are filled in epoxy resin of Material B. Material C is epoxy resin filled with irregular amorphous silica-particles and Material D is filled with globular amorphous silica-particles. In Materials B, C, and D, the silica-particles of 45 vol.% are included and their average particle size is about 33 μm. Young's modulus of the crystalline silica is 73.5 GPa and that of the amorphous silica is 76.3 GPa. Epoxy resins used were the circular fatty group and the acid anhydride was added to the epoxy resins as a hardening agent.

2.2 Impact fatigue test

Impact fatigue test was carried out using the rotary-disk-type impact fatigue testing machine. The details of this testing machine are described elsewhere[12]. The impact fatigue test was conducted at the stress ratio of 0.05-0.1 and a frequency of 10 Hz.

In this study, JIS K 7113 No. 3 specimen with 1-mm-deep V-notches machined mechanically on both sides of the straight portions was used. The specimen geometry and dimensions are shown in Fig. 1. This specimen is called the double-edge notched specimen. The crack gauge was placed on the V-notch tip of the specimen to measure the fatigue crack propagation velocity.

2.3 Usual fatigue test

The usual fatigue test (in this study, ordinary fatigue test is called "usual fatigue test" in order to distinguish it from the impact fatigue test) was carried out using the 1-ton-capacity servo electric-hydraulic fatigue testing machine at a stress ratio of 0.09 and a frequency of 10 Hz. The specimen geometry was the same as that for the impact fatigue test.

2.4 Tensile test

The specimen used was the same as the specimens used for the fatigue test except for the V-notches introduced on both sides of the straight portion of the specimen. The tensile test was carried out at a cross head speed of 0.05 mm/min using the Instron-universal testing machine. Young's modulus E and tensile strength σ_B were evaluated from the measured stress-strain curve.

2.5 Static fracture toughness test

Pre-cracked specimens, with the pre-cracks introduced at the tip of the slit, were used. The shape and dimensions of the slit specimen and the pre-cracked specimen are shown in Fig. 2. In this study, the pre-crack was introduced by applying the sustained load under the three-point-bending condition using the Instron-universal testing machine[13].

Static fracture toughness test was carried out based on the ASTM E399 method, with the Instron-universal testing machine at a cross head speed of 0.05 mm/min.

2.6 Dynamic fracture toughness test

Dynamic fracture toughness was evaluated with the instrumented Charpy impact test applying the impact response curve method presented by Kalthoff[11),(15)]. Capacity of the instrumented Charpy impact testing machine was 14.7 J and the test was conducted at an impact velocity of 0.5 m/sec which satisfies the

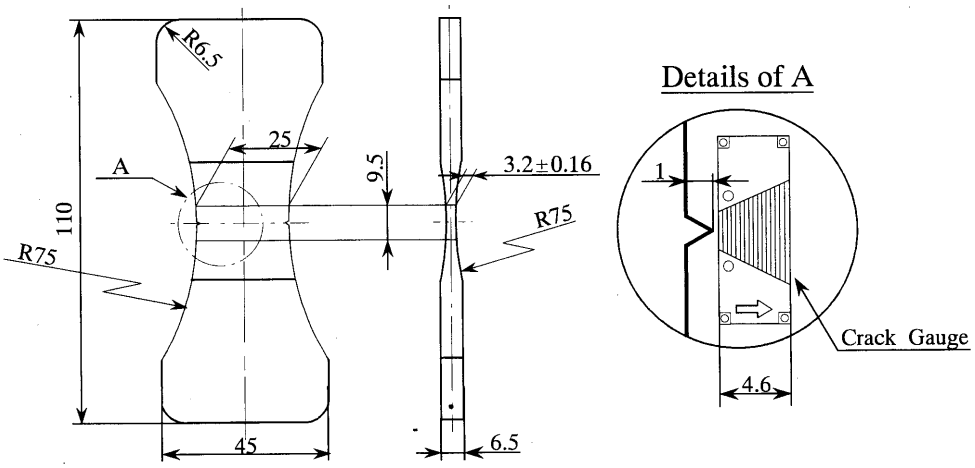

Fig. 1 Specimen geometry for impact and usual fatigue tests

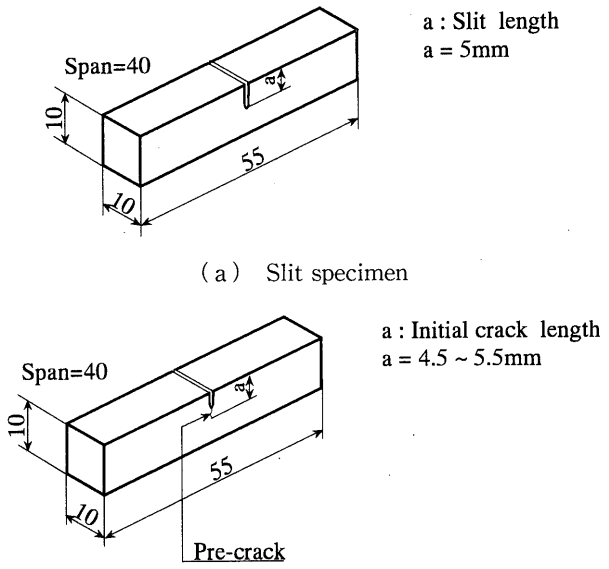

Fig. 2 Specimen geometries for dynamic (a) and static (b) fracture toughness tests and for instrumented Charpy impact test (c)

condition of $E_0 \geqq 3E_t$ (E_0 is applied energy and E_t is absorbed energy until fracture)[16]. The specimen used for recording the impact response curve was the slit specimen as shown in Fig. 2(a) and that for measuring the fracture time was the pre-cracked specimen as shown in Fig. 2(b).

2.7 Instrumented Charpy impact test

Instrumented Charpy impact test was carried out using the machine of 14.7 J capacity and the impact velocity was 0.5 m/sec which satisfies the $E_0 \geqq 3E_t$ condition. The specimen used was the U-notched one shown in Fig. 2(c). The load-deflection curve was recorded and the absorbed energy was analyzed by the CAI system[16),(17)].

The shape and dimensions of the specimen used for the dynamic fracture toughness test and the instrumented Charpy test are different from these of specimens generally used in the impact test of polymer materials. The shape and dimensions of the specimen used are based on the consideration of suppression of the vibrational wave generated at the impact[11)].

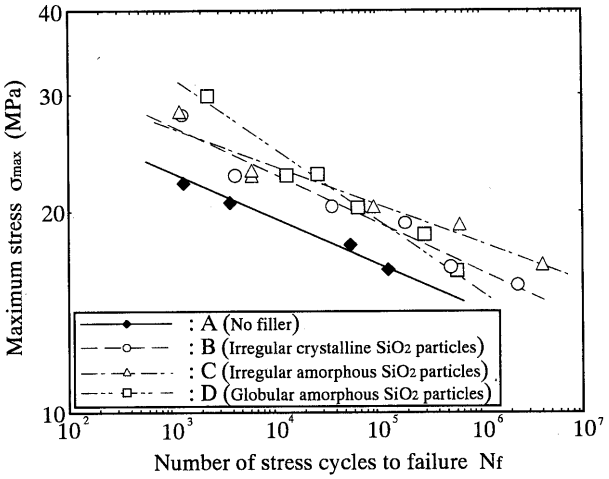

Fig. 3 S-N_f curves obtained from impact fatigue test

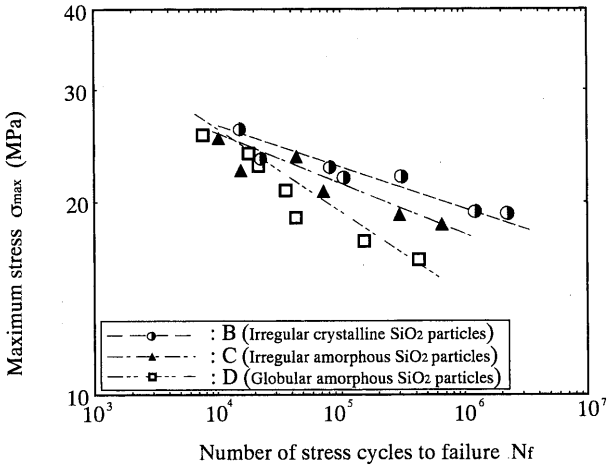

Fig. 4 S-N_f curves obtained from usual fatigue test

3. Results and Discussion

3.1 Impact fatigue properties and usual fatigue properties

The number of stress cycles to failure N_f can be divided into two numbers, that prior to crack initiation N_i, and that after crack initiation N_p. In this section, therefore, the impact fatigue test results are compared with the usual fatigue test results concerning (i) fatigue strength property (S-N_f curve), (ii) fatigue crack initiation property (S-N_i/N_f curve) and (iii) fatigue crack propagation property (ΔK-da/dN curve). In addition, the effects of silica-particle shape (globular or irregular) and silica-particle structure (crystalline or amorphous) on each fatigue characteristic are discussed.

3.1.1 Fatigue strength property (S-N_f curve)

Figure 3 shows the S-N_f curves obtained from the impact fatigue test and Fig. 4 shows the S-N_f curves obtained from the usual fatigue test. The following findings can be obtained from Figs. 3 and 4. 1) Effect

of filling with silica-particles: The impact fatigue resistance is improved by filling with silica-particles, as can be clearly seen in Fig. 3 from the fact that the S-N_f curves of Materials B, C and D lay on the upper side of that of Material A in the cycle range of $N_f = 10^3 - 10^6$. 2) Effect of silica-particle shape (globular or irregular): The comparison of Material C containing irregular amorphous silica-particles with Material D containing globular amorphous silica-particles indicates that the impact fatigue resistance of Material D is superior to that of Material C in the low cycle range of $N_f = 1\times10^3 \sim 5\times10^4$. On the contrary, in the high cycle range of $N_f = 5\times10^4 \sim 5\times10^6$, the impact fatigue resistance of Material C is superior to that of Material D. On the other hand, in the usual fatigue test, the fatigue resistance of Material C is superior to that of Material D in the range of $N_f = 10^4 \sim 10^6$. 3) Effect of silica-particle structure (crystalline or amorphous): The comparison of Material B containing irregular crystalline silica-particles with Material C containing irregular amorphous silica-particles indicates that the impact fatigue resistance of Material C is superior to that of Material B in both the low cycle and high cycle ranges. However, in the usual fatigue test, Material B shows superior fatigue strength. 4) In Materials B, C and D, the fatigue limit as normally observed in ferrous metallic materials could not be determined by either the impact or usual fatigue test.

The loading time T and the loading behavior of the impact fatigue test are different from these of the usual fatigue test. Therefore, it is difficult to evaluate the difference between the usual and impact fatigue behaviors only by comparing the S-N_f curves obtained by the two different tests. Consequently, the results shown in Figs. 3 and 4 are discussed using cumulative duration time defined by $N_f \times T$. The results are shown in Fig. 5. It is obvious in Fig. 5 that from the viewpoint of cumulative duration time significantly lower fatigue resistances were found in the impact fatigue tests for Materials B, C and D.

3.1.2 Fatigue crack initiation property (S-N_i/N_f curve) Figure 6 shows the relationship between N_i/N_f and σ_{max}. The crack initiation process dominates the fracture process when the N_i/N_f value is close to one. Conversely, the crack propagation process dominates the fracture process when the N_i/N_f value is less than one. The following findings concerning the fatigue crack initiation property were found. 1) The impact fatigue test results indicate that the N_i/N_f value do not change much and has a value of nearly one, with the exception of that for Material B at high stress level. This implies that the crack propagates unstably after the crack initiation and the final fracture is reached immediately. In contrast, in the usual fatigue test, the N_i/N_f values of Materials B, C and D decrease with increasing σ_{max}. This means that after the crack initiation a stable crack propagation stage is experienced by these materials. 2) The effect of silica-particle shape can be seen by comparing the S-N_i/N_f curve of Material C with that of Material D. The difference between the curves of these two materials in the usual fatigue test is more prominent than that in the impact fatigue test. This means that the silica-particle shape plays a more important role in the usual fatigue behavior than in the impact fatigue behavior. 3) The effect of silica-particle structure can be determined by comparing the S-N_i/N_f curve of the Material B with that of Material C. The difference in the curves of Materials B and C in the impact fatigue test is more pronounced than that in the usual fatigue test. This means that the silica-particle structure has a stronger influence on the impact fatigue behavior than on the usual fatigue behavior.

3.1.3 Fatigue crack propagation property (ΔK-da/dN curve) Although the double-edge notched

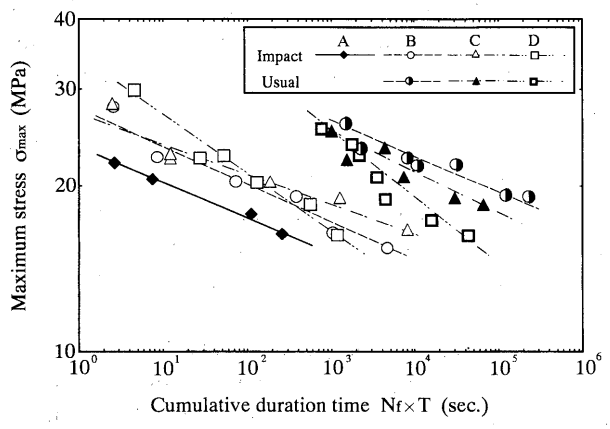

Fig. 5 S-$N_f \times T$ curves obtained from impact and usual fatigue tests

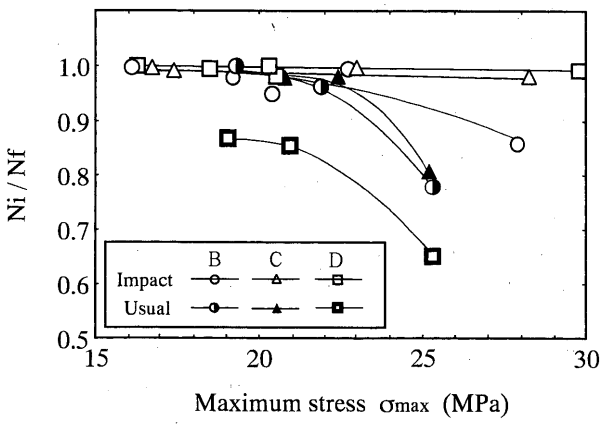

Fig. 6 S-N_i/N_f curves obtained from impact and usual fatigue tests

specimens are used for the fatigue tests as shown in Fig. 1, they are treated as single-edge notched specimen in the estimation of stress intensity factor. This is because of the fact that a fatigue crack always initiates from one side edge and the stress intensity factor range can therefore be estimated by Eq. (1)[18].

$$\Delta K=\Delta\sigma\sqrt{(\pi a)}\times F\left(\frac{a}{b}\right) \quad (1)$$

where, a is notch depth, b is specimen width and $F(a/b)$ is calculated from Eq. (2)[18].

$$F\left(\frac{a}{b}\right)=1.12-0.231\left(\frac{a}{b}\right)+10.55\left(\frac{a}{b}\right)^2-21.72\left(\frac{a}{b}\right)^3+30.39\left(\frac{a}{b}\right)^4 \quad (2)$$

On the other hand, measurement of the fatigue crack growth rate da/dN was carried out using the crack gauge placed onto the V-notch tip as mentioned in section 2.2.

Figures 7(a), (b) show the fatigue crack propagation properties (ΔK-da/dN curves) in the impact fatigue test and in the usual fatigue test, respectively. From Fig. 7, the following findings can be summarized. 1) In the order of the slope of ΔK-da/dN curve, the materials take place of Material B, Material D, Material C in the impact fatigue test. On the other hand, in the usual fatigue test, the order changes to Material B, Material C, Material D. 2) The effect of silica-particle shape on the ΔK-da/dN curve can be presented by comparing Material C with Material D. Material D exhibits superior impact fatigue to Material C and an opposite trend is found in the usual fatigue test. This indicates that the globular filler is a preferred for the impact fatigue propagation while the irregular filler is a preferred for the case of usual fatigue. 3) The effect of silica-particle structure on the ΔK-da/dN curve can be presented by comparing Material B with Material C. Material B with crystalline filler is a preferred for both impact fatigue crack propagation and usual fatigue crack propagation.

3.1.4 Fractography Figure 8 shows SEM fractographs at 400 μm away from the V-notch tip of the impact fatigue specimen. Figure 9 shows the SEM fractographs at 400 μm away from the V-notch tip of the usual fatigue specimen. These images of fracture surfaces are in the cycle range of $N_f=1\times10^5$ - 3×10^5. In Materials B and C, a pair of fracture surfaces are shown in Figs. 8 and 9. In the case of Material D, the fracture surface near the silica-particle is also shown at high magnification.

Concerning the impact and usual fatigue crack propagation behaviors, the followings conclusions can be made based on these SEM observations. 1) In both fatigue specimens, the exposed silica-particles are observed in the fracture surfaces of Materials B and C. This indicates that the fatigue cracks propagated by breaking through the silica-particles or the interfaces between silica-particle and epoxy resin matrix. 2) In both fatigue specimens, the exposed silica-particles cannot be observed at all in the fracture surface of Material D. This means that the fatigue cracks propagated through the epoxy resin matrix. 3) In Material D, the impact fatigue crack which detours forward the silica-particle continues straight after passing the silica-particle. However, the usual fatigue crack which detours forward the silica-particle after passing the silica-particle. These crack

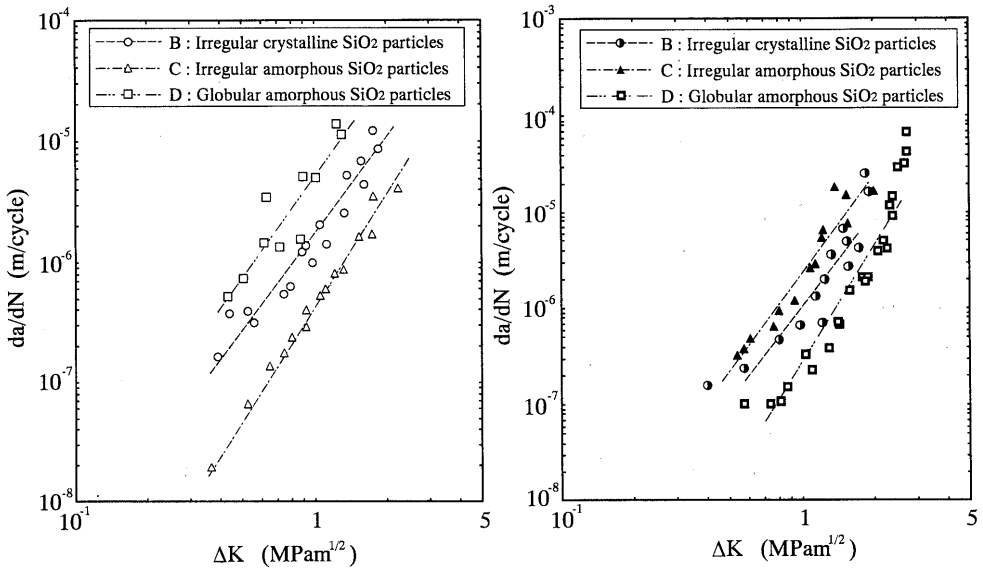

(a) Impact fatigue test (b) Usual fatigue test

Fig. 7 ΔK-da/dN relationships obtained from impact and usual fatigue tests

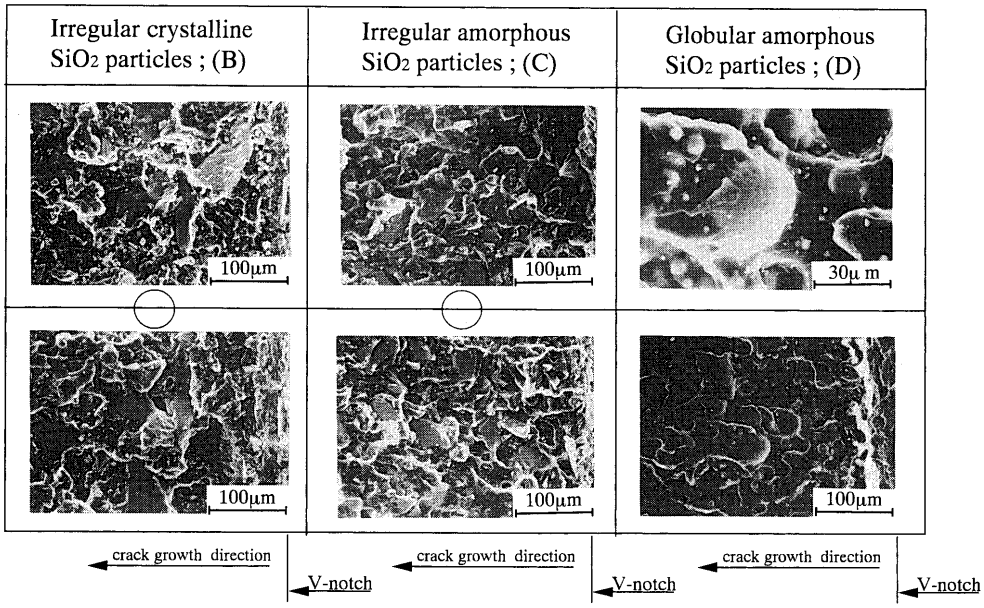

Fig. 8 SEM micrographs of typical impact fatigue fracture surfaces

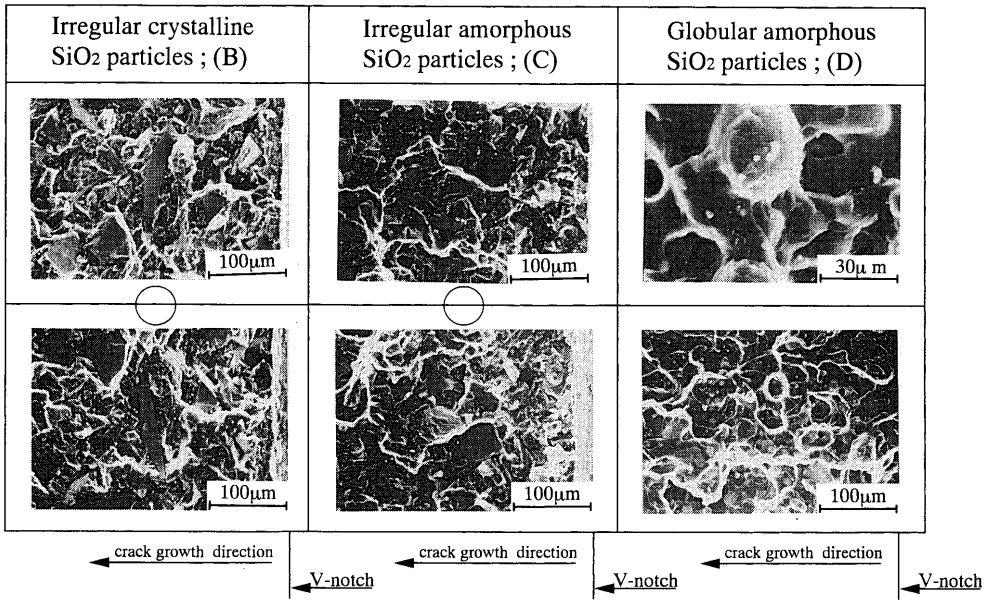

Fig. 9 SEM micrographs of typical usual fatigue fracture surfaces

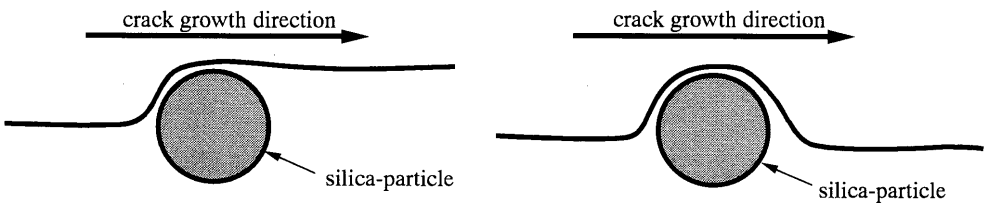

(a) Impact fatigue test (b) Usual fatigue test

Fig. 10 Schematic illustration of fatigue crack propagation modes for material D in impact and usual fatigue tests

propagation behaviors are schematically shown in Fig. 10. It is assumed that the difference in crack propagation rate between impact and usual fatigue tests is related to the above-mentioned difference in crack propagation behavior. While behaviors similar to these of 1) and 2) mentioned above have been

observed in the fracture surface of the dynamic fracture toughness test[13], the behavior of 3) is observed only in this study.

3.2 Synthetic evaluation of mechanical characteristics

In this section, mechanical characteristics are evaluated by considering the static mechanical properties such as Young's modulus E and tensile strength σ_B, fracture properties such as dynamic fracture toughness K_d, static fracture toughness K_s, fracture energy E_f and fatigue properties such as strength degradation constant m and power-exponent n in Paris's law. In this case, Young's modulus E represents the parameter of elastic deformation ability and the tensile strength σ_B is the parameter of resistance against the elastic-plastic deformation. The dynamic fracture toughness K_d is the parameter for fracture initiation under the dynamic loading condition, and the static fracture toughness K_s is that under the static loading condition. The fracture energy E_f is the energy consumed by only the fracture of specimen in the impact test of brittle materials and can be calculated from Eq.(3).

$$E_f = E_t - (E_k + E_m) \quad (3)$$

In Eq.(3), E_t is the absorbed energy until fracture, E_k is the kinetic energy that is spent to toss the broken specimen and E_m is the part consumed by the elastic deformation of testing machine. The details of the above analysis have been described in Refs.(11), (16) and (19).

The S-$N_f \times T$ curves can be formulated as shown in Eq.(4) and the strength degradation constant m is defined by Eq.(4)[12),(20)].

$$\sigma_{max} \times (N_f \times T)^m = D \quad (4)$$

where m is strength degradation constant, measures the degradation of strength due to fatigue damage, σ_{max} has been named as strength constant D when the cumulated loading time $N_f \times T$ equaled zero and reported to have some relationships with the tensile strength and the reduction of area in the case of steel[20].

Paris's law is represented as Eq.(5).

$$da/dN = C(\Delta K)^n \quad (5)$$

where constant n measures an increase in rate of crack propagation. In addition, suffix I indicates the impact fatigue test and suffix U indicates the usual fatigue test in the following context.

For Materials B, C and D, the Young's modulus E and the tensile strength σ_B are shown in Fig. 11. The dynamic fracture toughness K_d, the static fracture toughness K_s and the fracture energy E_f are shown in Fig. 12. Moreover, the strength degradation constant m and the power exponent n are compared for Materials B, C and D in Fig. 13. From Figs. 11, 12 and

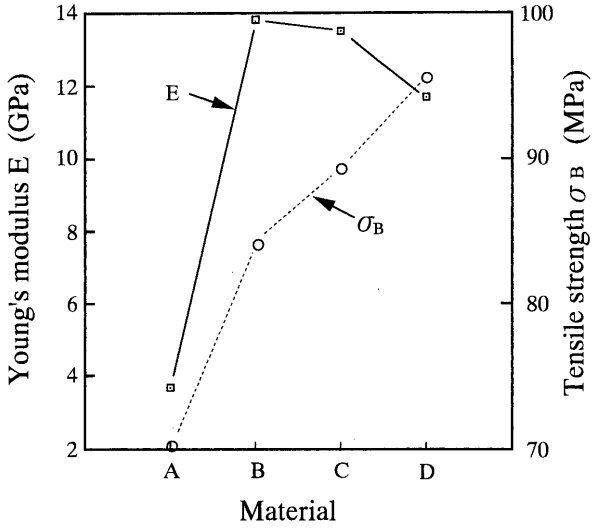

Fig. 11 Young's modulus E and tensile strength σ_B for various silica-particle characteristics

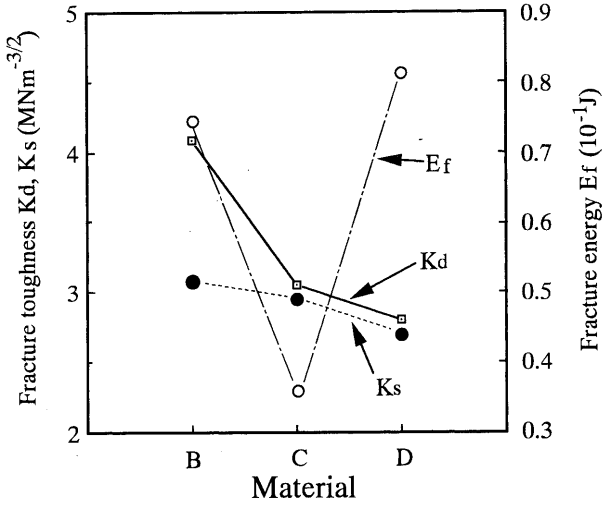

Fig. 12 Fracture characteristics for various silica-particle characteristics

13, all properties of Material B containing irregular crystalline silica-particles, Material C containing irregular amorphous silica-particles and Material D including globular amorphous silica-particles can be categorized as follows. 1) Properties in an increasing order of Material B<Material C<Material D are σ_B, m_U, n_U. 2) Properties in a decreasing order of Material B>Material C>Material D are E, K_d, K_s. 3) Properties in a decreasing order of Material D>Material B>Material C are, m_I, E_f. 4) Property in a decreasing order of Material C>Material D>Material B is n_I.

On the other hand, in addition to the above results, the influences of silica-particle characteristics can be summarized as follows. 1) The values of E, K_d, and K_s decreased with filling with the silica-particles as well as the values σ_B, M_U and n_U increased. 2)

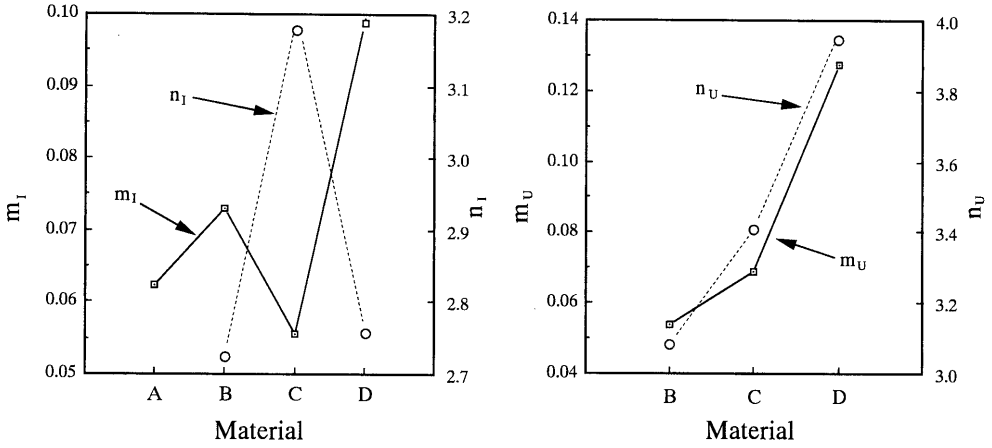

(a) Impact fatigue test (b) Usual fatigue test

Fig. 13 Fatigue characteristics for various silica-particle characteristics

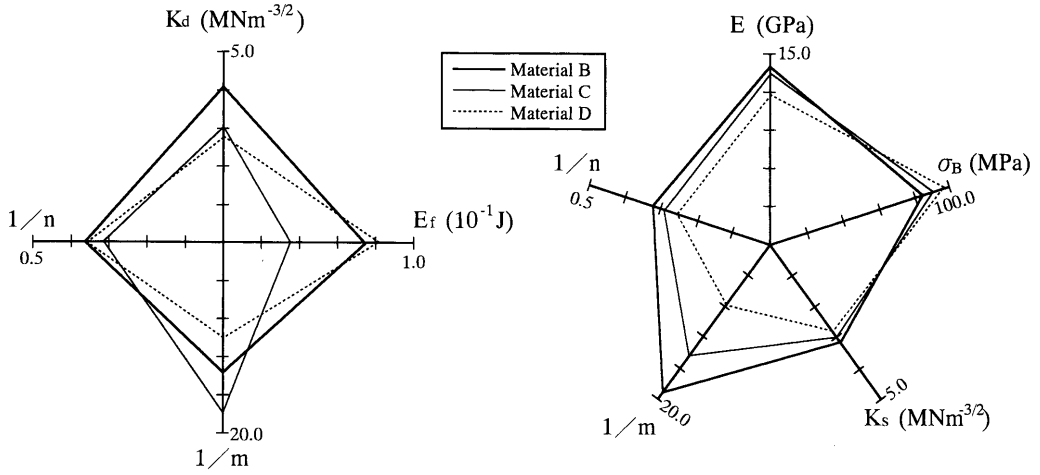

(a) Dynamic and impact (b) Static and usual

Fig. 14 Comparisons of mechanical characteristics

While the effect of the silica-particle characteristics on the fracture toughness of K_d and K_s are the same, their effects on the fatigue properties of the strength degradation exponent m and power exponent n in Paris's law are different.

As shown in Fig. 12, the change of fracture energy E_f does not correspond to those of dynamic fracture toughness K_d and static fracture toughness K_s. This may be attributed to the fact that the energy E_k spent to toss the broken specimen consumed by tossing specimen broken halves cannot be excluded perfectly from the fracture energy E_f.

Figure 14 shows the radar charts in which the above mentioned properties are plotted. For the radar charts it is assumed that the mechanical characteristics are good when the area enclosed by the lines connecting each property is large. It is also assumed that the balance of mechanical characteristics is good when the geometry of radar chart is nearly a circle. From the radar charts shown in Fig. 14, it is found that Material B containing the irregular crystalline silica-particles is the best among the materials tested having a good combination of mechanical characteristics.

4. Conclusions

The effects of shape (globular or irregular) and structure (crystalline or amorphous) of silica-particles in epoxy resin matrix on the impact/usual fatigue properties were investigated. The mechanical characteristics were evaluated synthetically from fatigue properties, tensile properties and fracture behaviors. Based on the experimental results the following conclusions can be drawn.

(1) The effects of silica filler in epoxy resin matrix on the impact/usual fatigue properties can be summarized as follows.

		fatigue	crack propagation
[structure]			
	impact	amorphous is good	crystalline is good
	usual	crystalline is good	crystalline is good
[shape]			
	impact	globular is good for $N_f=1\times10^3$~5×10^4 irregular is good for $N_f=5\times10^4$~5×10^6	globular is good
	usual	irregular is good	irregular is good

(2) The impact fatigue crack propagates unstably after crack initiation and reaches the final fracture immediately. On the other hand, the usual fatigue crack does not reach the final fracture immediately and a stable crack propagation is obtained.

(3) Concerning the crack initiation behavior, the silica-particle shape shows a pronounced effect on the usual fatigue property. On the other hand, the particle structure shows a marked effect on the impact fatigue property.

(4) The filling of silica-particle in resin increases σ_B, m_U and n_U of the material, and decreases the values of E, K_d and K_s. The silica-particle characteristics shows a similar effect on the fracture toughness of K_d and K_s. Their effects on the fatigue properties of the strength degradation exponent m and power exponent n in Paris's law are different.

(5) Material B containing the irregular crystalline silica-particles is the best material among those tested having combination of good mechanical characteristics.

References

(1) Nishimura, A., Yaguchi, A. and Kawai, A., J. of the Soc. of Mat. Sci., (in Japanese), Vol. 38, No. 434 (1989), pp. 1322-1328.

(2) Yaguchi, A., Nishimura, A. and Kawai, S., J. of the Soc. of Mat. Sci., (in Japanese), Vol. 40, No. 452 (1991), pp. 554-560.

(3) Nishimura, A. and Yaguchi, A., J. of the Soc. of Mat. Sci., (in Japanese), Vol. 41, No. 466 (1992), pp. 1054-1059.

(4) Yaguchi, A. and Nishimura, A., J. of the Soc. of Mat. Sci., (in Japanese), Vol. 42, No. 472 (1991), pp. 40-45.

(5) Nakamura, Y., Yamaguchi, M., Kitayama, A., Okubo, M. and Matsumoto, T., Polymer, Vol. 32, No. 12 (1991), pp. 2221-2229.

(6) Nakamura, Y., Yamaguchi, M., Okubo, M. and Matsumoto, T., Polymer, Vol. 32, No. 16 (1991), pp. 2976-2979.

(7) Nakamura, Y., Yamaguchi, M., Okubo, M. and Matsumoto, T., J. of Applied Polymer Science, Vol. 44 (1992), pp. 151-158.

(8) Nakamura, Y., Yamaguchi, M., Okubo, M. and Matsumoto, T., Polymer, Vol. 33, No. 16 (1992), pp. 3415-3426.

(9) Nakamura, Y., Yamaguchi, M., Okubo, M. and Matsumoto, T., J. of Applied Polymer Science, Vol. 45 (1992), pp. 1281-1289.

(10) Nakamura, Y., Yamaguchi, M. and Okubo, M., Polymer Eng. and Sci., Vol. 33, No. 5 (1993), pp. 279-284.

(11) Yamamoto, I., Miyata, H. and Kobayashi, T., JSME Int. J. Ser. I, Vol. 35, No. 3 (1992), pp. 361-366.

(12) Niinomi, M., Uwai, K., Kobayashi, T. and Okahara, A., Eng. Frac. Mech., Vol. 38, No. 6 (1991), pp. 439-449.

(13) Igakura, S., Yamamoto, I., Kobayashi, T. and Higashihara, T., J. of the Mat. Sci. of Japan, (in Japanese), Vol. 29, No. 6 (1992), pp. 307-315.

(14) Niinomi, M., Kobayashi, T., Uwai, K., Ohishi, T. and Higashihara, T., Mech. Behav. Mat. VI, Vol. 2 (1991), pp. 549-555.

(15) Kalthoff, J.F., Int. J. Frac., Vol. 33 (1987), p. 209.

(16) Kobayashi, T., Yamamoto, I. and Niinomi, M., J. of Testing and Evaluation, Vol. 21, No. 3 (1993), pp. 145-153.

(17) Yamamoto, I. and Kobayashi, T., J. Pres. Ves. & Piping, Vol. 55 (1993), pp. 295-312.

(18) Shiratori, M., Miyoshi, T. and Matsusita, H., Suuchihakairikigaku, (in Japanese), (1981), p. 75, Jikkyou-shuppan.

(19) Kobayashi, T., Niinomi, M., Koide, Y. and Matsunuma, M., Trans. JIM, Vol. 27, No. 10 (1986), pp. 775-783.

(20) Nakayama, H. and Tanaka, M., J. of the Soc. of Mat. Sci., (in Japanese), No. 387, Vol. 34 (1989), pp. 1483-1489.